Stability Analysis and Adaptive Resonance Damping of Multi-Converter System Applying Bidirectional Converter

Roosa-Maria Sallinen
Tampere University
Tampere, Finland
roosa.sallinen@tuni.fi

Tomi Roinila
Tampere University
Tampere, Finland
tomi.roinila@tuni.fi

Hessamaldin Abdollahi
University of South Carolina
Columbia, USA
abdollh@email.sc.edu

***Abstract*—Bidirectional converters have become extensively applied in various dc power systems that contain battery energy storage systems (BESSs). Such dc power systems typically consist of several feedback-controlled converters, forming a complex power distribution system. Consequently, a number of stability issues arise due to interactions among multiple converter subsystems. Recent studies have presented adaptive control methods for guaranteeing the stability of a multi-converter system under varying operating conditions. However, most methods have not fully considered the bidirectional power-flow in BESS that significantly affects the system dynamics and stability analysis. This paper demonstrates how a bidirectional converter can be operated as an adaptive virtual impedance to improve overall system performance. In the method, an adaptive resonance term is added to the converter's voltage controller to damp resonances in the network's bus impedance, thus improving voltage damping and guaranteeing stability. The reliability and performance of the multi-converter system can be maintained under varying operating conditions by updating the bidirectional converter controller structure so that the required bus voltage damping level is guaranteed.**

***Index Terms*—adaptive stabilization, dc power systems, resonance-based controller, bidirectional converter, multi-converter system**

I. INTRODUCTION

Battery energy storage systems (BESSs) have an increasingly important role in many power-distribution systems, such as aircrafts, ships, and dc micro grids [1]–[3]. The operation of these systems often depends on a bidirectional power-electronics converter, which enables bidirectional power-flow and controls the charge and discharge processes of the energy storage.

Typically, the bidirectional converter is a part of a larger system consisting of several converters connected to a common dc bus, as shown in Fig. 1. Such a system may often experience performance degradation or instability due to impedance interactions between different converters although the converters may operate well in a standalone mode. The controller of each converter in the network is designed to track either a voltage, current, or power reference. The high bandwidth of the load converters introduces a negative incremental impedance at the point of coupling with the dc bus, and the load converters

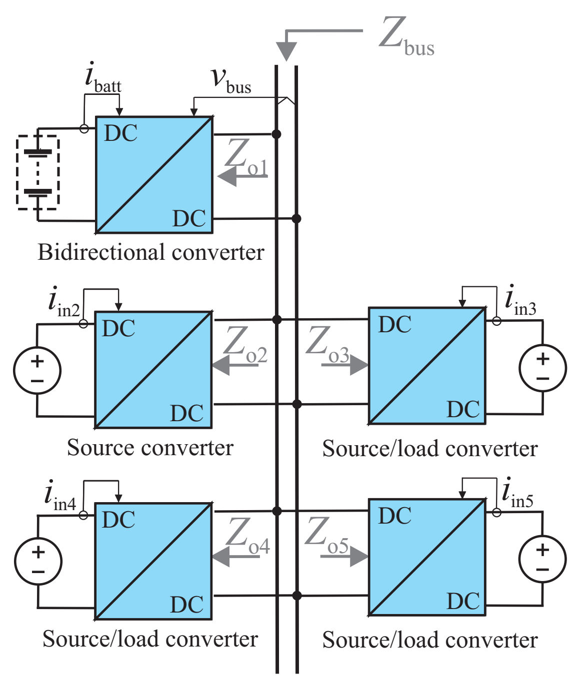

Fig. 1. Dc-dc source and load converters connected to the same bus with a bidirectional dc-dc converter.

are typically represented as constant power loads (CPLs). The negative incremental impedance of CPLs is known to present a destabilizing effect on the system [4] and it is the main reason of interaction dynamics in dc multi-converter systems [5], [6]. Therefore, in a multi-converter system, the stability cannot be reliably evaluated by only studying the operation of single converters.

Typical methods to assess the stability or performance of a converter system are based on minor-loop-gain defined as the ratio between the source subsystem output impedance and the load subsystem input impedance. Examples of such methods include Middlebrook criterion, gain-margin and phase-margin criterion, passivity criterion, and pole location visualization. These methods are, however, not directly applicable to systems including bidirectional power-flow because the methods require that the subsystems and system grouping are clearly defined and formulated [7]. A different approach to analyze the stability of a multi-converter system is to apply the minor-loop gain based on the converter role in contributing to the current and voltage control instead of characterizing the converters as load and source converters [8]. However, as the control roles may also change based on the operating modes of the applications, this method may not be applicable for all multi-converter systems. A passivity-based stability analysis based on bus impedance was proposed in [7]. The method requires only the bus-impedance information, which is independent of the power-flow directions, the converter operation modes, and system grouping, making it suitable for multi-converter systems with bidirectional power-flow.

One method to avoid impedance-based system performance degradation caused by the CPLs is adding passive/active circuit components to the existing system [5], [9]. However, adding new components can increase both cost and size of the overall system and/or slow down the voltage response [10]. Hence, modifying the feedback loops of the individual converters without adding any extra components is a more attractive solution.

Methods that aim to mitigate the impedance-based interactions by changing the converter control structure are often separated into two groups: the load-side stabilizing methods and the source-side stabilizing methods. In the methods, either the output admittance of the CPL is reshaped using specific control solutions, [6], [10], [11], or control solutions are used to change the output admittance of a source converter, [12]–[14]. For most of the active-damping methods on the load side, the stabilizing damping controller deteriorates the converter load performance and slows down the converter output dynamics. Therefore, control solutions on the source side have been considered more efficient. In [13], a virtual negative inductor is used on the source-side converter by using the droop control method, thus enhancing the system damping effect. As the implementations are either on the source- or load-side converter, they cannot be implemented on bidirectional converters.

Different control methods that aim to mitigate the impedance-based interactions by changing the control structure of converters with bidirectional power-flow have been implemented in [5] and in [15]–[17]. In [5], a feedback control of an energy storage is used to increase the robustness of the system by mitigating the transients which occur due to temporary faults at the dc bus. In [15], a control method for multiple bidirectional power converters is proposed to reduce the circulating current and power-sharing deviation among converters of a hybrid ac/dc microgrid in island mode. Virtual impedance -based method is implemented for a multi-converter system with an AC/DC converter and a battery in [16]. Droop control with virtual impedance is implemented on bidirectional converters in [17].

An adaptive stabilization method which utilizes bus impedance measurements is implemented on a source-side converter in [18]. As the bus impedance method is based on impedance measurements, it is possible to monitor the system stability in real time and to utilize adaptive controllers [18]–[20]. However, these studies have not applied bidirectional converters for reshaping the impedance. Even though the bus impedance method allows for a straightforward stability and performance analysis of a system with bidirectional converters, the internal converter dynamics change along the changing power-flow direction. When implementing the stabilizing control on a bidirectional converter, these changes in the dynamics should be addressed to ensure that the virtual impedance design does not lead to a degradation in the bidirectional converter's internal performance, possibly leading to instability.

This paper extends the stability and performance studies of multi-converter systems presented in [18] and [19] by implementing the stabilizing control using a bidirectional converter. Such a converter can act as a source or load converter, depending on its operation mode. Specifically, the limitations of implementing the stabilizing controller on a bidirectional converter instead of a source converter are discussed. It is shown that the impedance of the bidirectional converter can be adjusted to reach a desired level of system damping in both load- and source-operation modes by applying the measured bus impedance to implement the adaptive virtual impedance. This can be achieved regardless of possible variations in the applications or operating modes.

The remainder of the work is organized as follows. In Section II, the bus impedance -based stability and performance analysis of a multi-converter system is presented. In Section III, the resonance damping control method is presented and its effect on the voltage controller is discussed. In addition, the process of obtaining bus impedance measurements and updating the resonance damping control parameters is described. In Section IV, simulations are conducted for validating the effectiveness of the resonance controller on a bidirectional converter operating both as a load and as a source. Finally, the conclusions are drawn in Section V.

II. Theory and Methods

A. Performance Assessment Based on Bus Impedance

In order to implement an adaptive controller that can guarantee a desired damping level for the system, a measurable performance assessment method is required. A straightforward method to assess the performance and stability of a multi-converter system with bidirectional power-flows and changing control modes is based on analyzing a parameter called bus impedance [21]. For a system with N converters connected to a common bus, the bus impedance Z_{bus} can be given as a parallel connection of the impedances as

$$Z_{\mathrm{bus}}(s) = \frac{1}{Z_{\mathrm{o1}}^{-1} + Z_{\mathrm{o2}}^{-1} + ... + Z_{\mathrm{oN}}^{-1}}, \quad (1)$$

where N impedances are measured on the corresponding subsystem's bus-side (indicated with subscript o in Fig. 1) and positive current direction is defined as flowing into the converter. Note that as the direction of the power-flow does not affect the definition, the method is suitable for systems with bidirectional power-flows as well as changing operating modes and structures [7]. These terminal impedances describe the terminal behaviour of the subsystem around certain operating point.

In order to address the stability of the interconnected system, two requirements should be met in order to obtain passivity (and therefore stability) [21]:

1) $Z_{\rm bus}(s)$ has no right half plane (RHP) poles
2) Re$\{Z_{\rm bus}(j\omega)\} \geq 0, \forall\omega > 0$, i.e. arg$\{Z_{\rm bus}(j\omega)\} \in [\pm 90^o]$

The second condition states that the system is passive (and therefore stable) if the bus impedance ($Z_{\rm bus}$) phase stays within $\pm 90^o$.

The passivity is only a sufficient but not a necessary requirement for the stability, and therefore, further concepts are required to address the performance metrics. To this end, allowable impedance region (AIR), introduced in [22], can be used. The AIR is defined as a semicircle in the right-half side of the complex plane wherein $Z_{\rm bus}(s)$ should be located to achieve a specified system damping level.

Typically, the system bus impedance is dominated by a single large resonant peak [22]. Hence, the impedance can be simplified into a form

$$Z_{\rm bus}(j\omega) = Z_{\rm o-bus}\frac{s\omega_{\rm o}}{s^2 + s\omega_{\rm o}/Q_{\rm bus} + \omega_{\rm o}^2}, \quad (2)$$

where $Z_{\rm o-bus}$ is the characteristic impedance of $Z_{\rm bus}$ with a resonance frequency $\omega_{\rm o}$ and the quality factor $Q_{\rm bus}$ specifying the level of damping of $Z_{\rm bus}$ at $\omega_{\rm o}$. Hence, at $\omega_{\rm o}$ (i.e. at the frequency where the bus impedance phase is 0^o), $Z_{\rm bus}(j\omega_{\rm o}) = Z_{\rm o-bus}Q_{\rm bus}$, which means that the bus impedance has a real value, and it describes the resonance peak magnitude at the least damped frequency $\omega_{\rm o}$. To achieve a specified system damping level, the AIR requires that the bus impedance has to achieve a specified quality factor, $Q_{\rm max}$. In the complex plane, the AIR can be given as a semicircle with a specified radius $Z_{\rm o-bus}Q_{\rm max}$. To simplify the comparison, the results can be normalized by dividing both the bus impedance and the radius with the characteristic impedance $Z_{\rm o-bus}$, leading to a clear representation of the AIR as a semicircle with a radius $Q_{\rm max}$. Therefore, if the normalized bus impedance $Z_{\rm bus-N}(j\omega)$ stays within the AIR, the specified level of damping is achieved.

B. Typical Bus Impedance Characteristics

The dynamic behavior of a typical bus impedance based on Eq. 2 is shown in Fig. 2. Based on Eq. 1, the bus impedance increases when its denominator becomes smaller. The bus-side impedance of a CPL can be described as a negative incremental impedance within the feedback control loop bandwidth, i.e., its magnitude is resistive and phase is -180^o. On the other hand, the bus-side impedance of a voltage-controlling converter can be described as having very low impedance at low frequencies. However, the impedance has a resonance around the voltage control cross-over frequency, which causes the magnitude to peak. This peak may cause the parallel sum of the CPL impedances and the voltage controlling converter

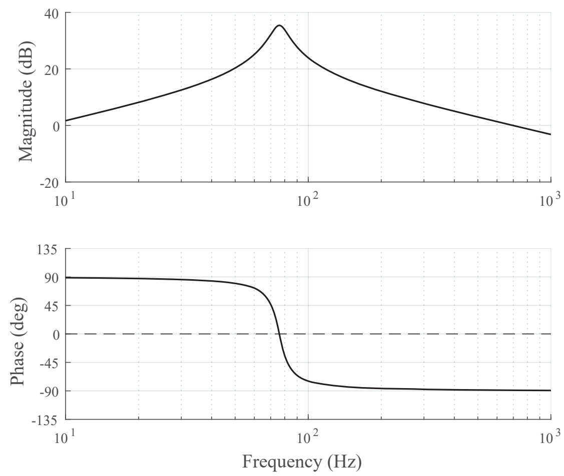

Fig. 2. Frequency response of the bus impedance as given in Eq. 2 with $Z_{\rm o-bus} = 9$, $\omega_{\rm o} = 477$ rad/s, and $Q_{\rm bus} = 6.5$.

impedance to have equal or comparable magnitudes at a frequency close to the voltage control cross-over frequency. Furthermore, if the phase difference between the impedances is greater than 180^o at this frequency, the denominator in Eq. 1 becomes very small and the bus impedance exhibits a large resonant peak. This phenomena is an example of impedance-based interactions within a multi-converter system and should be taken into account when analyzing the system stability and performance.

It is intuitive that a possible resonance or instability caused by the impedance-based interactions can be prevented by adding a virtual impedance on the voltage controlling converter's impedance, damping the resonance in the bus impedance. Even though the resonance behavior could also be smoothed by, for example, increasing the converter's bus-side capacitance, a control-oriented solution would be more desirable as extra hardware would add cost as well as slow down the dynamics, leading to a non-optimized solution under some operating points, for example, at lower powers.

It is well known that the resonance (peak) in the voltage controlling converter's impedance is caused by a resonant pole, and it occurs close to the voltage control cross-over frequency. Therefore, it is typical that the resonance of the bus impedance occurs at a frequency slightly lower than the voltage control loop bandwidth.

III. Adaptive Control of Bidirectional Converter for Resonance Damping

A. Resonance Damping Control

To prevent impedance-based interactions from degrading the system performance, the impedance(s) can be reshaped so that a specific damping level is guaranteed. As a result, the converters in the network do not interact with each other in an adverse way.

The goal is to modify the converter control so that the closed-loop impedance is further damped in a range around

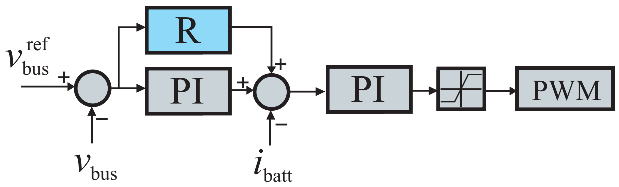

Fig. 3. Block diagram of the converter controller with a resonance term.

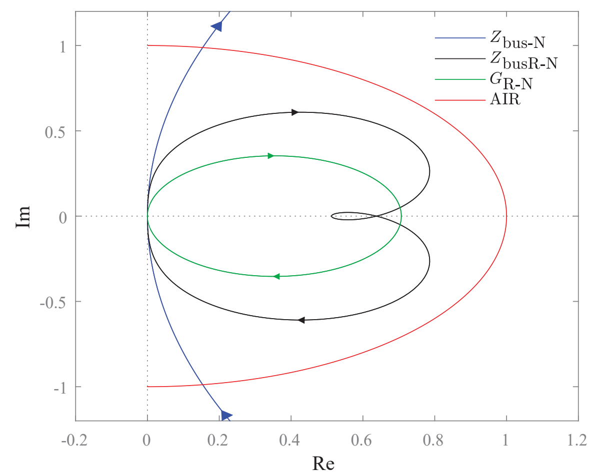

Fig. 4. Normalized bus impedance without R-gain (blue line) and with R-gain (black line), normalized R-gain (green line), and AIR boundary (red line) with Q_{d} = 0.7, $Q_{\max}$ = 1, K_{m} = 0.5. Bus impedance as given in Eq. 2 with $Z_{\mathrm{o-bus}} = 9$, $\omega_{\mathrm{o}} = 477$ rad/s, and $Q_{\mathrm{bus}} = 6.5$.

the resonance. Specifically, the following design requirements should be met:

- the resulting normalized bus impedance $Z_{\mathrm{bus-N}}(j\omega)$ stays within the AIR which is specified as a semicircle with a radius of maximum allowed quality factor $Q_{\max}$ on the complex plane,
- the resulting normalized bus impedance at the resonance frequency $Z_{\mathrm{bus-N}}(j\omega_{\mathrm{o}})$ has an extra separation margin K_{m} guaranteeing a safe distance from the AIR boundary $Q_{\max}$, and
- the added virtual impedance itself has a damping corresponding to the chosen quality factor Q_{d}.

Typical ranges for these parameters are $Q_{\max} = 0.7...1$, $K_{\mathrm{m}} = 0...1$, and $Q_{\mathrm{d}} = 0.7...1$. To meet these criteria, the voltage controlling converter's bus-side impedance can be reshaped by adding a damping term to its voltage control loop. To this end, a resonance gain (R-gain) is added in parallel with the voltage controller, given as [23]

$$G_{\mathrm{R}} = \frac{2K_{\mathrm{r}}\omega_{\mathrm{r}}s}{s^2 + 2\omega_{\mathrm{r}}s + \omega_{\mathrm{o}}^2}, \tag{3}$$

where K_{r} determines the amount of damping at the resonance frequency ω_{o} and ω_{r} is the bandwidth of the resonance. A block diagram of the controller structure is given in Fig. 3, where the converter is under a cascaded control with an outer voltage loop providing reference to an inner current loop, which controls the battery current i_{batt}.

Measurements of the bus impedance can be utilized to determine sufficient values for the parameters K_{r}, ω_{r}, and ω_{o} so that the design requirements are met. In [18], the relation between the parameters of the R-gain and the design requirements are derived as:

$$K_{\mathrm{r}} = \frac{Q_{\mathrm{d}}}{Z_{\mathrm{o-damp}}}; \omega_{\mathrm{r}} = \frac{\omega_{\mathrm{o}}}{2Q_{\mathrm{d}}}, \tag{4}$$

where

$$Z_{\mathrm{o-damp}} = Z_{\mathrm{o-bus}}\frac{Q_{\mathrm{d}}Q_{\mathrm{bus}}\left(Q_{\max} - K_{\mathrm{m}}\right)}{Q_{\mathrm{bus}} - \left(Q_{\max} - K_{\mathrm{m}}\right)}, \tag{5}$$

and the resonance frequency ω_{o} can be directly identified from the bus impedance.

The R-gain improves the damping of the bus-impedance, hence improving the system performance and stability. An illustrative example is given in Fig. 4, where the normalized bus impedance is presented with and without R-gain. Also the added R-gain is presented after normalizing it by multiplying the gain by $Z_{\mathrm{o-damp}}$. Without the R-gain, the bus impedance has a quality factor around 6 (out of scale). An addition of the R-gain results in a normalized bus impedance which stays within the AIR, thus guaranteeing the required damping level. At the resonance frequency, the damping equals $Q_{\max} - K_{\mathrm{m}}$, as required, to guarantee a safe distance from the AIR boundary. Furthermore, the added virtual impedance itself has a damping corresponding to the chosen quality factor Q_{d}. Hence, all the requirements have been met.

The control method based on R-gain is demonstrated in [18] for a source buck converter. When operating with a load converter, the power-flow direction is the opposite. As the bus impedance is not dependent on the power-flow direction, this does not affect the fundamental idea behind the control design. However, since the converter dynamics change, this may cause issues for the voltage controller stability or performance if the R-gain affects the voltage control loop in a degrading manner.

B. *Effect of R-Gain on Voltage Control*

The nominal voltage control gain (PI) is typically designed based on the desired crossover frequency f_{c} and phase-margin φ_{m}. In this work, the converter that performs the stabilization is considered to be a bidirectional dc-dc converter shown in Fig. 5. The detailed transfer functions can be found in [24]. The current controller and voltage controller are both based on PI strategy and the voltage controller is given by $G_{\mathrm{v-PI}}(s) = K_{\mathrm{p-v}} + K_{\mathrm{i-v}}/s$. When the R-gain is added to the controller, is becomes $G_{\mathrm{v-PI-R}}(s) = G_{\mathrm{v-PI}}(s) + G_{\mathrm{R}}(s)$.

An example of the effect of the R-gain on the voltage controller gain is presented in Fig. 6, where the voltage controller gain is shown with and without the R-gain. Also the R-gain is shown. The R-gain parameters are $K_{\mathrm{r}} = 0.5$, $\omega_{\mathrm{r}} = 80 * 2\pi$ rad/s, and $\omega_{\mathrm{o}} = 80 * 2\pi$ rad/s, and the PI-gain parameters are $K_{\mathrm{p-v}} = 0.55$ and $K_{\mathrm{i-v}} = 704$. It can be seen

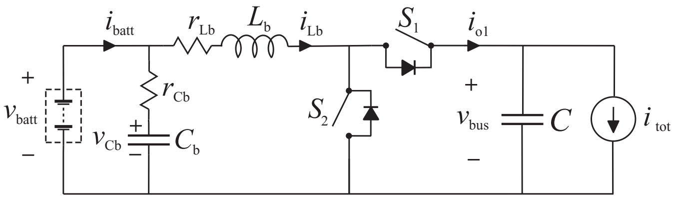

Fig. 5. Bidirectional dc-dc converter.

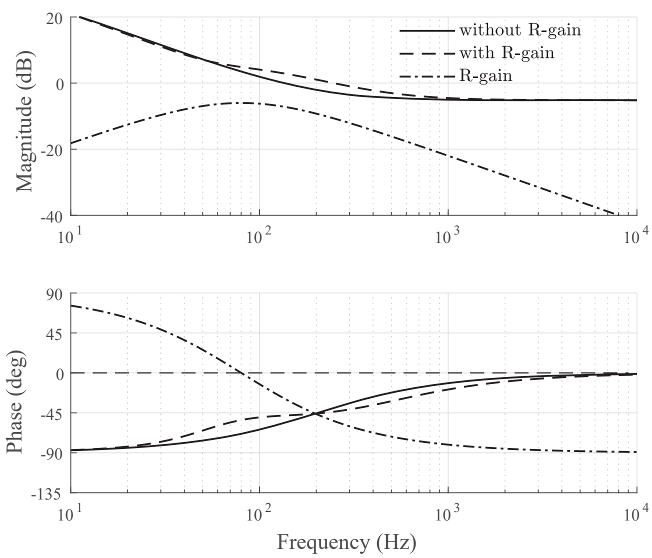

Fig. 6. Frequency response of the voltage controller without (G_{PI}) and with damping ($G_{\text{PI-R}}$) and the damping R-gain (G_{R}).

that the added R-gain has an effect only around the resonance frequency.

The effect of the R-gain on the original (PI) controller performance is small. However, since the R-gain increases the voltage control gain in the specified range, its effect on phase margin and cross-over frequency should be taken into account to make sure that the resonance term does not degrade the normal operation of the controller. For example, too wide R-gain bandwidth may increase the voltage control loop cross-over frequency too much because the stable operation is limited both by the inner loop control bandwidth (the inner and outer loop should be decoupled in a cascaded controller) and possible poles or zeros in the converter dynamics. In the case of a bidirectional converter, this is especially important as the system dynamics, specifically, the locations of the system poles and zeros, typically change profoundly when the power direction changes (e.g. buck vs. boost converter). By taking these restrictions into account in the design, the controller can damp possible resonances in the bus impedance without internal voltage control performance degradation.

C. Bus Impedance Measurements

Since the dynamics of the multi-converter system may change over time and can be difficult to predict, adaptive damping controller is most desired. Accordingly, bus impedance is a suitable performance assessment as it can be measured periodically by means of wideband measurement techniques [25]. By injecting a broadband excitation such as a pseudorandom binary sequence (PRBS) to the converter control (system input) signals and measuring the resulting currents and bus voltage (system output signals), and processing these input and output signals with Fourier techniques, the bus impedance can be constructed. Based on the acquired bus impedance, the controller can react to the changes in the network. This process is represented as a flowchart in Fig. 7. Note that it is often enough to measure the bus impedance only around the voltage control cross-over frequency. Furthermore, to achieve faster adaptive response from the controller, methods based on orthogonal binary sequences can be applied to speed up the bus-impedance identification procedure [19].

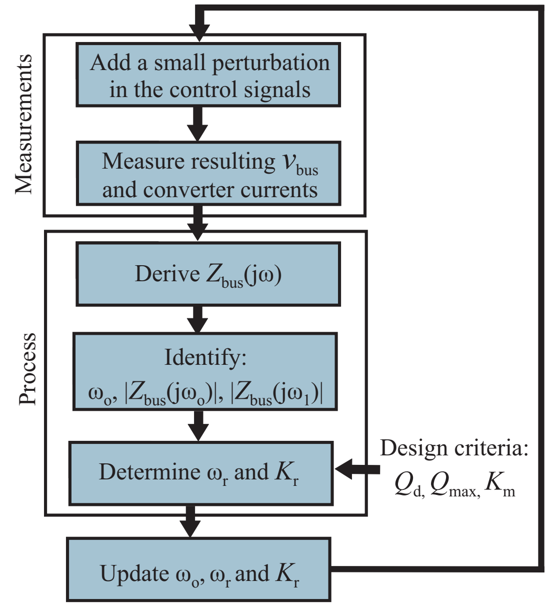

Fig. 7. Flowchart representing the adaptive resonance damping algorithm.

The greatest advantage of the impedance-based method is its black box feature: detailed knowledge of the parameters and properties of the system are not required as long as the impedance measurement can be performed [26]. The drawbacks of the impedance-based stability assessment include inability to identify the causes of the instability or resonance without further analysis. Nonetheless, the method offers enough information to adapt the virtual impedance according to the changes in the network, and hence the resonance can be prevented regardless of its root-cause.

IV. Simulation results

This section demonstrates the ability of the control algorithm to damp the resonances caused by interactions among the different converters in a multi-converter system both in charging and discharging mode. The network corresponds to the structure given in Fig. 1. The topology of the bidirectional converter is shown in Fig. 5, where the current direction is assumed

TABLE I
CONVERTER PARAMETERS FOR THE BIDIRECTIONAL CONVERTER (BC) AND THE OTHER CONVERTERS (C2-C5) IN FIG. 1.

Parameters	Values (BC / C2-C5)	Description
V_{bus}	480 V	bus voltage
V_{in}	350 V / 200 V	battery/voltage source voltage
f_{sw}	20 kHz	switching frequency
C	85 μF / 45 μF	bus-side capacitance
r_{C}	250 mΩ / 100 mΩ	bus-side capacitor ESR
L	1 mH	inductance
r_{L}	3.6 mΩ	inductor ESR
C_{b}	1 μ F	input-side capacitance
r_{Cb}	10 mΩ	input-side capacitor ESR
r_{sw}	10 mΩ	switch on-time resistance
$f_{\mathrm{c-c}}$	2 kHz	current loop cross-over frequency
$\varphi_{\mathrm{m-c}}$	65^o / 60^o	current loop phase margin
$f_{\mathrm{c-v}}$	100 Hz / none	voltage loop cross-over frequency
$\varphi_{\mathrm{m-v}}$	55^o / none	voltage loop phase margin

TABLE II
OPERATING MODES FOR THE BIDIRECTIONAL CONVERTER (BC) AND THE OTHER CONVERTERS (C2-C5) IN FIG. 1.

BC operating mode	BC	C2	C3	C4	C5
source	30 kW	15 kW	-15 kW	-15 kW	-15 kW
load	-30 kW	15 kW	-15 kW	15 kW	15 kW

positive in discharging mode [24]. The other converters share the same topology, but are here designated as source- or load-converters. All the controllers utilize a PI control strategy. The bidirectional converter controls the battery current and the bus voltage using cascaded control with and without the damping R-gain, while the other converters control just their input side currents. The converter parameter values are given in Table I. In this example all the converters are standalone stable, and therefore, the possible degradation in system performance originates from the interactions between single converters. The R-gain parameters are chosen based on bus impedance Z_{bus} and Eq. (4) with Q_{d} = 0.5, $Q_{\max}$ = 1, and K_{m} = 0.5.

Two situations are simulated: the converter is either discharging (source mode) or charging (load mode) the battery. The converter operating modes for both cases are given in Table II, where negative power indicates that the converter operates as a load. The time-domain results are shown in Fig. 8 for the source mode and in Fig. 9 for the load mode, with and without the resonance damping R-gain. In the source mode, it is clear that without the R-gain there occurs a resonance around 70 Hz. In the load mode, the resonance is smaller but can still be identified at 70 Hz.

The corresponding bus impedances are shown in Fig. 10, with and without the resonance damping R-gain. The R-gain indeed increases the resonance damping. The resonance occurs around 70 Hz in both cases. The Nyquist contours of the corresponding normalized bus impedances are shown in Fig. 11 which indicate that the resulting normalized bus impedances stay within the AIR boundary, thus guaranteeing the desired damping level.

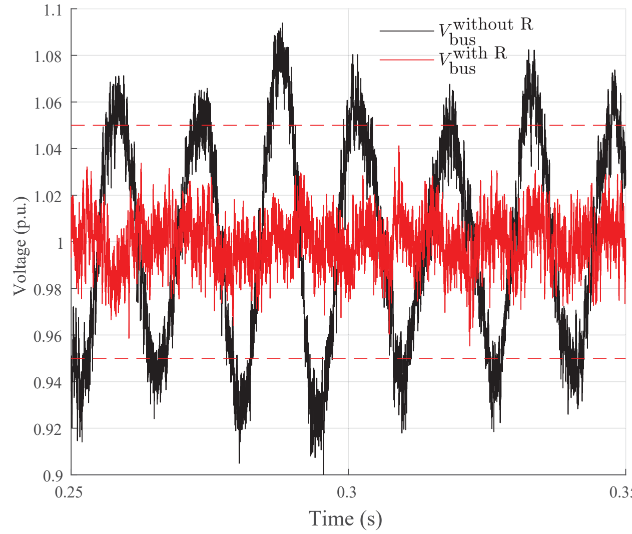

Fig. 8. Bus voltage with and without damping in discharging mode (i.e. source).

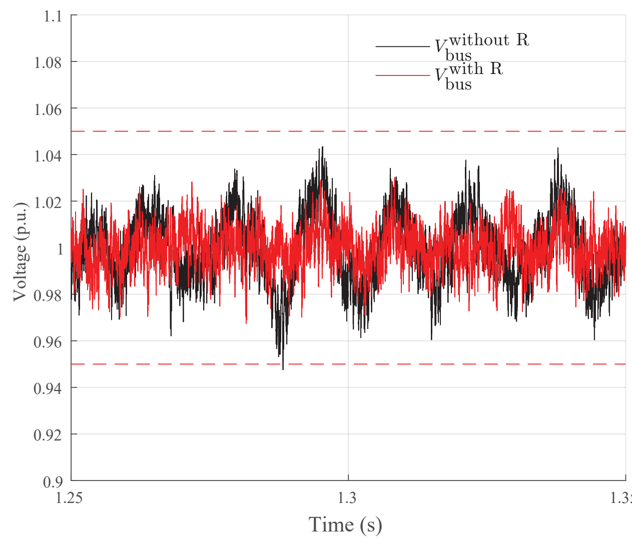

Fig. 9. Bus voltage with and without damping in charging mode (i.e. load).

V. CONCLUSION

This paper has utilized a bidirectional converter to provide adaptive damping in a multi-converter system. The adaptive tuning of the resonance controller is based on bus impedance measurements, which are used to estimate the system's stability and performance. Using the data from these bus impedance measurements, the bidirectional converter is operated as a virtual impedance, damping resonances in the bus impedance. The analysis shows that the bidirectional converter can efficiently damp the resonances in the bus impedance. As a result, the reliability and performance of the network can be maintained regardless of possible network or operating mode changes and without hardware updates or controller re-tuning.

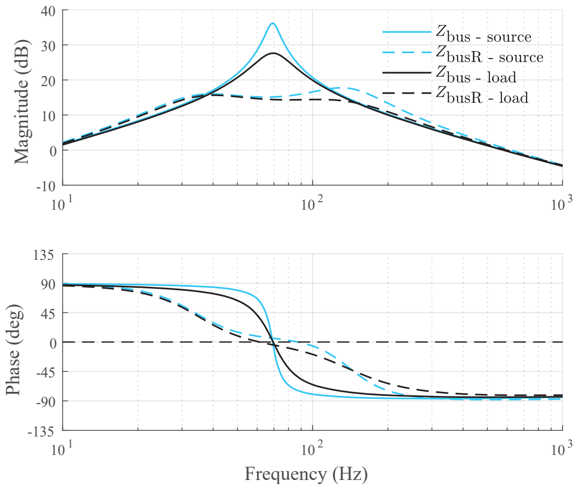

Fig. 10. Bus impedance with and without damping R-gain both in discharging (source) and charging (load) mode.

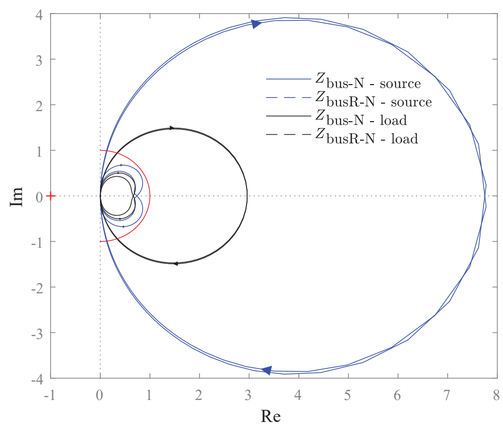

Fig. 11. Bus impedance with and without damping R-gain both in discharging (source) and charging (load) mode. AIR boundary indicated with the red line.

References

[1] H. Zhang, F. Mollet, C. Saudemont, and B. Robyns, "Experimental validation of energy storage system management strategies for a local dc distribution system of more electric aircraft," *IEEE Transactions on Industrial Electronics*, vol. 57, no. 12, pp. 3905–3916, Dec 2010.

[2] Z. Jin, L. Meng, J. M. Guerrero, and R. Han, "Hierarchical control design for a shipboard power system with dc distribution and energy storage aboard future more-electric ships," *IEEE Transactions on Industrial Informatics*, vol. 14, no. 2, pp. 703–714, Feb 2018.

[3] T. K. Roy, M. A. Mahmud, A. M. T. Oo, M. E. Haque, K. M. Muttaqi, and N. Mendis, "Nonlinear adaptive backstepping controller design for islanded dc microgrids," *IEEE Transactions on Industry Applications*, vol. 54, no. 3, pp. 2857–2873, May 2018.

[4] Xiaogang Feng, Jinjun Liu, and F. C. Lee, "Impedance specifications for stable dc distributed power systems," *IEEE Transactions on Power Electronics*, vol. 17, no. 2, pp. 157–162, 2002.

[5] L. Herrera, W. Zhang, and J. Wang, "Stability analysis and controller design of dc microgrids with constant power loads," *IEEE Transactions on Smart Grid*, vol. 8, no. 2, pp. 881–888, 2017.

[6] X. Lu, K. Sun, J. M. Guerrero, J. C. Vasquez, L. Huang, and J. Wang, "Stability enhancement based on virtual impedance for dc microgrids with constant power loads," *IEEE Transactions on Smart Grid*, vol. 6, no. 6, pp. 2770–2783, 2015.

[7] A. Riccobono and E. Santi, "Comprehensive review of stability criteria for dc power distribution systems," *IEEE Transactions on Industry Applications*, vol. 50, no. 5, pp. 3525–3535, Sep. 2014.

[8] X. Zhang, X. Ruan, and C. K. Tse, "Impedance-based local stability criterion for dc distributed power systems," *IEEE Transactions on Circuits and Systems I: Regular Papers*, vol. 62, no. 3, pp. 916–925, March 2015.

[9] M. Cespedes, L. Xing, and J. Sun, "Constant-power load system stabilization by passive damping," *IEEE Transactions on Power Electronics*, vol. 26, no. 7, pp. 1832–1836, 2011.

[10] W. Lee and S. Sul, "Dc-link voltage stabilization for reduced dc-link capacitor inverter," *IEEE Transactions on Industry Applications*, vol. 50, no. 1, pp. 404–414, Jan 2014.

[11] B. A. Martinez-Treviño, A. E. Aroudi, A. Cid-Pastor, and L. Martinez-Salamero, "Nonlinear control for output voltage regulation of a boost converter with a constant power load," *IEEE Transactions on Power Electronics*, vol. 34, no. 11, pp. 10 381–10 385, 2019.

[12] M. Wu and D. D. Lu, "A novel stabilization method of lc input filter with constant power loads without load performance compromise in dc microgrids," *IEEE Transactions on Industrial Electronics*, vol. 62, no. 7, pp. 4552–4562, 2015.

[13] S. Liu, P. Su, and L. Zhang, "A virtual negative inductor stabilizing strategy for dc microgrid with constant power loads," *IEEE Access*, vol. 6, pp. 59 728–59 741, 2018.

[14] X. Zhang, Q. Zhong, V. Kadirkamanathan, J. He, and J. Huang, "Source-side series-virtual-impedance control to improve the cascaded system stability and the dynamic performance of its source converter," *IEEE Transactions on Power Electronics*, vol. 34, no. 6, pp. 5854–5866, June 2019.

[15] H. Xiao, A. Luo, Z. Shuai, G. Jin, and Y. Huang, "An improved control method for multiple bidirectional power converters in hybrid ac/dc microgrid," *IEEE Transactions on Smart Grid*, vol. 7, no. 1, pp. 340–347, 2016.

[16] J. He, L. Du, B. Liang, Y. Li, and C. Wang, "A coupled virtual impedance for parallel ac/dc converter based power electronics system," *IEEE Transactions on Smart Grid*, vol. 10, no. 3, pp. 3387–3400, 2019.

[17] P. Yang, M. Yu, Q. Wu, N. Hatziargyriou, Y. Xia, and W. Wei, "Decentralized bidirectional voltage supporting control for multi-mode hybrid ac/dc microgrid," *IEEE Transactions on Smart Grid*, vol. 11, no. 3, pp. 2615–2626, 2020.

[18] H. Abdollahi, S. Arrua, T. Roinila, and E. Santi, "A novel dc power distribution system stabilization method based on adaptive resonance-enhanced voltage controller," *IEEE Transactions on Industrial Electronics*, vol. 66, no. 7, pp. 5653–5662, July 2019.

[19] T. Roinila, H. Abdollahi, S. Arrua, and E. Santi, "Real-time stability analysis and control of multiconverter systems by using mimo-identification techniques," *IEEE Transactions on Power Electronics*, vol. 34, no. 4, pp. 3948–3957, April 2019.

[20] S. K. Gurumurthy, M. Cupelli, and A. Monti, "A generalized framework for synthesizing virtual output impedance control of grid integrated power electronic converters," in *2018 IEEE International Conference on Power Electronics, Drives and Energy Systems (PEDES)*, Dec 2018, pp. 1–6.

[21] A. Riccobono and E. Santi, "A novel passivity-based stability criterion (pbsc) for switching converter dc distribution systems," in *2012 Twenty-Seventh Annual IEEE Applied Power Electronics Conference and Exposition (APEC)*, Feb 2012, pp. 2560–2567.

[22] J. Siegers, S. Arrua, and E. Santi, "Stabilizing controller design for multibus mvdc distribution systems using a passivity-based stability criterion and positive feedforward control," *IEEE Journal of Emerging and Selected Topics in Power Electronics*, vol. 5, no. 1, pp. 14–27, March 2017.

[23] D. N. Zmood and D. G. Holmes, "Stationary frame current regulation of pwm inverters with zero steady-state error," *IEEE Transactions on Power Electronics*, vol. 18, no. 3, pp. 814–822, May 2003.

[24] R. Sallinen, T. Messo, and T. Roinila, "Mitigating voltage fluctuations in battery energy storage systems," in *2019 20th Workshop on Control and Modeling for Power Electronics (COMPEL)*, 2019, pp. 1–6.

[25] T. Roinila, T. Messo, R. Luhtala, R. Scharrenberg, E. C. W. de Jong, A. Fabian, and Y. Sun, "Hardware-in-the-loop methods for real-time frequency-response measurements of on-board power distribution systems," *IEEE Transactions on Industrial Electronics*, vol. 66, no. 7, pp. 5769–5777, July 2019.

[26] G. O. Kalcon, G. P. Adam, O. Anaya-Lara, S. Lo, and K. Uhlen, "Small-signal stability analysis of multi-terminal vsc-based dc transmission systems," *IEEE Transactions on Power Systems*, vol. 27, no. 4, pp. 1818–1830, Nov 2012.